Enhancing Solar Irradiance Estimation for Pumped Storage Hydroelectric Power Plants Using Hybrid Deep Learning

Sudharshan Konduru[1], C. Naveen [1,*], Ramesh C. Bansal [2,3,*]

[1] Department of Electrical and Electronics Engineering, SRM Institute of Science and Technology, Kattankulathur, Chennai 603203, India

[2] Electrical Engineering Department, University of Sharjah, Sharjah, United Arab Emirates

[3] Electric, Electronic and Computer Engineering Department, University of Pretoria, Pretoria, South Africa

*Correspondence to:

C. Naveen. Email: leonaveen173@gmail.com or Ramesh C. Bansal. Email: rcbansal@ieee.org

Abstract

This research article explores the potential of Pumped Storage Hydroelectric Power Plants across diverse locations, aiming to establish a sustainable electric grid system and reduce per-unit energy costs. A distinctive feature of the study involves forecasting solar irradiance on large-scale hydroelectric dam locations to identify optimal sites for a PV-integrated hydropower system. The research focuses on advancing the integration of floating solar power modules on water storage systems in eight selected regions across India, emphasizing precise solar irradiance estimation. The paper introduces a state-of-the-art hybrid intelligent deep learning model, combining time series analysis and deep learning through residual ensembling to address these challenges. The primary objective is to pinpoint the optimal location for a Power Storage System (PSS) with the highest solar irradiation for PV-integrated hydro system integration. A secondary goal involves minimizing errors within computational time constraints by the proposed model. The study also employs various optimization techniques to enhance its effectiveness and fine-tune the model's performance, contributing to the advancement of sustainable energy solutions. The proposed model performs best with a Whale optimization algorithm with mean absolute error varying from 0.34 to 3.63 W/m^2 and root mean square error from 0.75 to 9.51 W/m^2 on PSS locations. The analysis also confirms average solar irradiance is high on PSS 7 with 221.0 W/ m^2 followed by PSS 1 with 221.1 W/ m^2 among the eight designated sites.

Keywords: Pumped storage systems; Solar irradiance forecasting; PV integrated hydro systems; Whale optimization algorithm

Introduction

Sustainable and green power generation is required to fulfil the increasing global energy demand and keep the planet carbon neutral. The potential utilization of renewable resources like solar, hydro, tidal, wind, etc. can help achieve this [1]. Solar energy is the most alluring of these potential renewable energies owing to its ubiquity and technological development. India, on average, receives annual solar radiation of 200 MWh/km², presenting a substantial

opportunity for effectively utilizing and harnessing solar to fulfil the country's electricity requirements [2]. However, due to the solar energy intermittent nature, an energy storage system is required to provide load power during the absence of photovoltaic (PV) power [3]. As a result, integrating appropriate storage technology with the PV system improves the system's reliability and efficiency [4]. The market now offers a variety of storage alternatives. However, India, with its extensive network of streams and rivers, has considerable potential for hydroelectricity storage systems. India also has small-scale hydro energy facilities spread throughout the nation that provide electricity for rural and off-grid regions. By July 2023, India has installed 50.07 GW from large hydropower plants (above 25 MW capacity) and 4.8 GW from small hydropower plants [5]. At present, progress in the hydro energy sector has been relatively low and has experienced certain hurdles [6]. Delays in completing projects, ecological issues connected to large-scale dams, challenges related to land procurement, and rehabilitation of displaced people are among the Hurdles. Hence, the hydro system can serve as a storage facility to improve the reliability of solar power and electrical demands. Similar facilities for PV-integrated hydropower are available across the country through pumped storage systems. There will be enhanced system reliability facilitated by grid connectivity through transmission lines and transformers. Apart from this, there will be an increase in power generation with low expenditure.

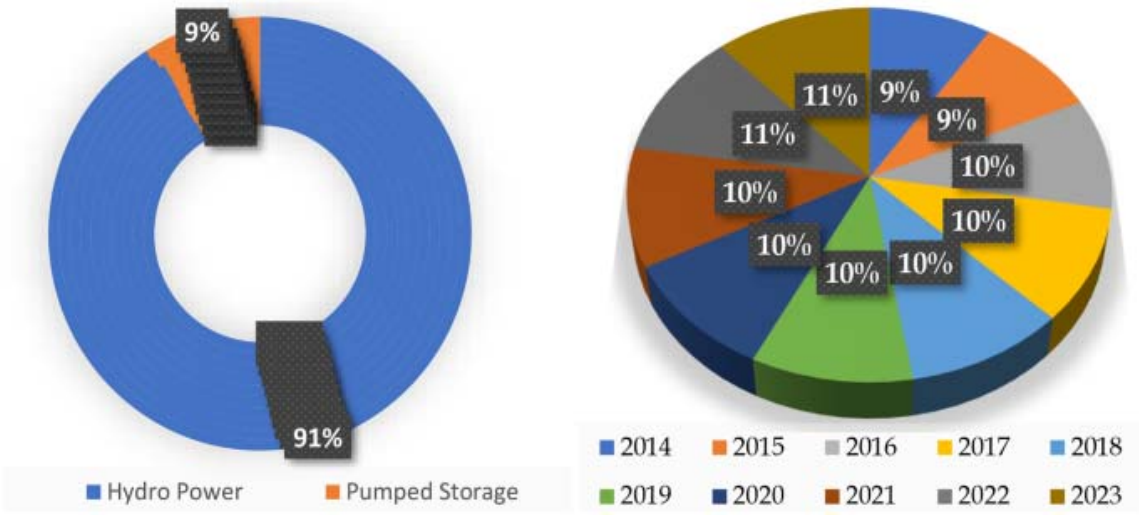

Fig. 1. (**a**) PSS hydropower in Hydro Energy (**b**) Pumped Storage Hydropower capacity/year

Figure 1(a) and 1 (b) show the power generation capacity enhancements of pumped Storage systems in the total hydro-energy systems and year-wise capacity installations for the world from 2014 to 2023 respectively [7]. Run of River, Storage, Multipurpose, and Pumped Storage are four types of hydropower generation [8]. This research centers on diverse storage technologies with an emphasis on novel technologies related to pumped hydro energy storage. The study explores various possibilities for integrating renewable energy and balancing the grid. The overarching goal is to delineate a cost-effective and sustainable roadmap that facilitates high-level integration [9]. Pumped storage plants [10] serve as hydraulic energy storage devices, offering a crucial role in grid-based energy storage. Considered the primary large-scale option for power utilities in design and economics, pumped storage technology involves pumping water from a lower reservoir to an upper reservoir during periods of excess electricity, utilizing off-peak hours or reduced demand. When additional electricity is required, water from the upper reservoir is released back to the lower reservoir through a turbine [11]. A

reversible pump-turbine machine, such as a Reversible Francis Turbine, can operate as both a pump and a turbine. Consequently, the PSS system has a negative net generation balance as it consumes more energy to pump the water uphill than it generates when the water flows down from the upper reservoir [12].

This plant stands out for its quick start-up time, sustainability, scalability, and economic feasibility for large-scale power generation, making it a desirable choice for HRES projects [13]. It is not ideal to have separate storage at every renewable energy site in India, with its connected power grid. Doing so can be costly. So many places worldwide are choosing grid-connected Pumped Hydro Energy Storage (PHES) systems. This decision helps shift electric energy time, leveling loads, and making energy use more efficient.

Figure 2 shows the solar irradiance on the PSS locations with their hydropower capacities in India. Two (Kadana, Sardar Sarovar RBPH) from Gujarat, Two (Nagarjuna (N J) Sagar) from Andhra Pradesh, Two (Ghatgarh, Bhira) from Maharashtra, One (Kadamparai) from Tamil Nadu, and the final one (Purulia) from West Bengal [14]. The mean day ahead solar irradiance in Fig. 2 is calculated by analyzing the 40 years of day ahead NASA power database renewable energy data.

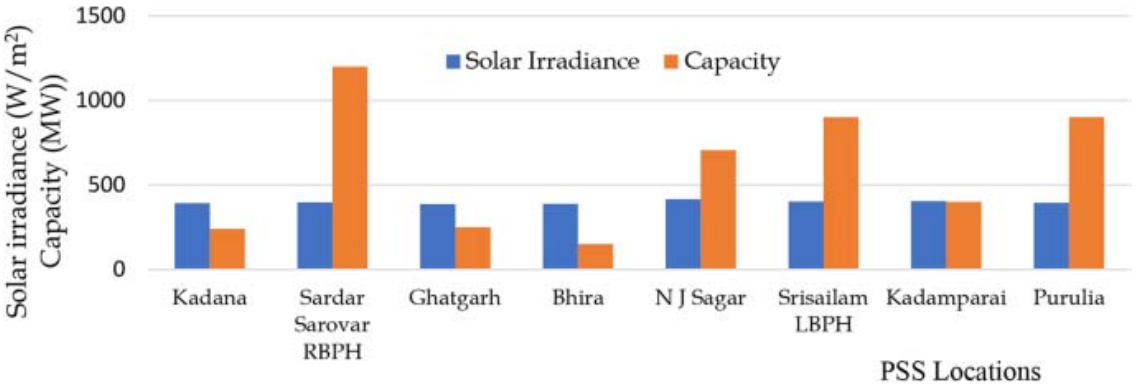

Fig. 2. Day ahead Solar irradiance on Pumped Storage systems in India

Efficient operations of PV-integrated hydroelectric power plants require a thorough understanding and management of the relationship between solar energy and the hydro system [15]. Solar irradiance faces variability and uncertainty due to complex interactions with atmospheric components. The temporal and spatial variations in factors like water vapor, aerosols, and clouds contribute to this uncertainty, impacting solar power generation reliability [16]. Therefore, the direct penetration of solar power into electricity markets introduces grid instability, requiring a real-time balance between generation and consumption. Challenges include unpredictable ramps, forecast errors, and intra-hour variability. Solutions like grid-wide power storage or accurate solar forecasts for grid regulation and power scheduling are essential to address solar variability.

Related Literature

Increasing demands for solar integration into smart grids have led to diverse forecasting methodologies [17]. Forecasting models generate predictions for solar irradiance or active power output [18] and vary based on seasonal, geographic, and meteorological factors, making direct comparisons challenging [19, 20]. The inputs for these models vary, and selecting

appropriate inputs is a crucial step in their development. General inputs for solar forecasting include features from sky images, local meteorological data, and historical irradiance data [21]. Data-driven forecasting models establish mathematical relationships between observations and predictions through training data [22]. These methods offer advantages such as fault tolerance, minimal prior assumptions, applicability to both linear and nonlinear datasets, and high-speed performance [23]. Due to these benefits, data-driven approaches are used widely for forecasting applications. It ensures numerical consistency, improves data stability, and facilitates the object-to-data mapping process. However, the diverse characteristics of irradiance time series under various weather conditions necessitate training data that spans a broad range, encompassing all possible seasonal and meteorological scenarios for efficient model training, optimization, and evaluation [24].

Solar forecasts frequently handled as time-series predictions resulted in ARMA (Auto Regressive Moving Average) and ARIMA (Auto Regressive Integrated Moving Average) models' utilization in solar forecasting applications [25]. Deep learning methods are proving to be extremely beneficial in solar prediction, as they can independently decipher complicated patterns from raw data and uncover complex relationships that are not easily recognizable with conventional statistical approaches [26]. These models offer the opportunity to improve prediction accuracy and forecasting capabilities [27]. Deep learning methods, notably Artificial Neural Networks (ANN), are commonly used for solar irradiance forecasts due to their ability to handle complex nonlinear interactions. The Multilayer Perceptron (MLP) has been introduced as an established ANN structure to predict intra-hour Global Horizontal Irradiance (GHI), Direct Normal Irradiance (DNI), and PV power generation [28]. With advances in deep learning, Recurrent Neural Networks (RNNs) such as Long Short-Term Memory (LSTM) and Gated Recurrent Unit (GRU) have been used to assess and forecast the sequence or time series of irradiance [29].

Several LSTM architectures are trained to estimate solar irradiance using historical data, demonstrating LSTM's ability to capture intricate patterns accurately in time series data [30]. Stacked LSTMs, which reflect more complex functions than a single hidden layer of LSTM neurons, are also used for irradiance predictions [31]. Although LSTMs have competitive accuracy in solar irradiance forecasting, their adoption is hampered by significant training times [32]. Therefore, GRUs are used for short-term PV generation projections to shorten training times without sacrificing accuracy [33]. Machine and Deep learning methods are prominent strategies for solar forecasts, yet they have certain limitations. Hence hybrid models are required to reduce the uncertainties by reducing the limitations. The fusion of conventional methods with artificial intelligence techniques provides researchers and practitioners with diverse tools to tackle the challenges of solar forecasting [34]. This approach makes it possible to explore different methods and identify the most suitable techniques for specific tasks based on data characteristics and desired accuracy levels. In parallel, various studies have investigated the application of residual ensembling models in solar prediction. ARIMA model proves adept at providing residuals from time series data, while deep neural networks excel at modeling long-range dependencies [35].

Optimizers serve a vital role in the training phase of deep neural networks (DNNs), influencing the adjustment of synaptic weights. They control the degree of modification to the gradient of the activation function, thereby shaping the entire training process. The optimizer updates node synaptic weights to minimize error, with guidance from the cost function directing it towards the optimal path to reach global minima [36]. Here is an example, Sunanda et al. propose optimization models based on the Grasshopper Optimization Algorithm (GOA) [37] and the

Moth Flame Optimization (MFO) algorithm [38]. These models aim to increase convergence speed, account for non-linearity, and minimize power generation costs for short-term hydrothermal scheduling (HTS) integrating solar and wind energy [39]. In the same way, effective tuning of deep learning model hyper-parameters is critical for optimizing solar irradiance forecasting performance in the current research for integrating solar and hydro energy, leading to the use of Whale optimization algorithm (WOA), Bayesian optimization algorithm (BOA), Particle swarm optimization algorithm (PSOA), and Genetic algorithm (GA).

The study introduces a hybrid deep learning model based on GRU for time series forecasting, utilizing a twenty-three-year hour-based dataset from eight PSS locations in India. The main objectives of our work are.

1. Forecasting the solar irradiance on the eight PSS locations in India for installing floating solar power modules on the water storage systems.
2. Developing a hybrid intelligent deep learning model based on residual ensembling using the advantages of Time series and Deep learning models.
3. Optimum selection of maximum solar irradiance PSS location for placement of the PV integrated hydro system.
4. Enhancing the performance of the developed model with various optimization algorithms.

Data Processing

Three pieces of information are required in the work. First, hydropower data was taken from the Energy Ministry of India, second, the latitude and longitude locations of the PSS were taken from Global Energy Monitor (GEM) websites, and the final solar irradiance data was taken from NASA renewable energy power database [40]. A total of eight PSS sites namely Kadana, Sardar Sarovar RBPH, Ghatgarh, Bhira, N J Sagar, Srisailam LBPH, Kadamparai, and Purulia in India. All places require grid integration, so the location data is obtained from the GEM wiki. Based on location data, the irradiance data (0 to 24 h) with a minimum of fifteen feature selections of twenty-three years are downloaded from the NASA database. For each location, it took twelve downloads, and for eight locations, it took ninety-six downloads. This data is filtered, processed, and arranged in sequence from 2001 January to 2023 October with total data of nearly two lakhs in each location forming eight datasets.

Theories and Methods

The main aim of the research is to introduce an intelligent hybrid deep learning model to predict solar irradiance. The proposed work contains the Bi–GRU model, ARIMA model, and different optimization algorithms to enhance the accuracy of the proposed model.

Proposed Methodology

The available eight-location data after data processing is passed through the Augmented Dickey-Fuller test to optimize the parameters for the ARIMA model by splitting each data based on the train/test ratio. Then the split data from the PSS location is first passed into the optimized ARIMA time series forecasting model. This makes the time series data stationary and ensures good predictions from the ARIMA model. The output residues from the ARIMA model are passed into the Bi-GRU model. The optimization models such as PSOA, WOA,

BOA, and GA are used thereby to update the hyperparameters like batch size, epoch number, neuron number, and learning rate for the Bi–GRU model. The same is repeated for the remaining seven PSS locations.

Finally, the mean solar irradiance from predictions in each location is chosen and verified to select the optimal location to integrate the PV power in the hydro system. The flow chart in Fig. 3 shows the work process of the proposed methodology.

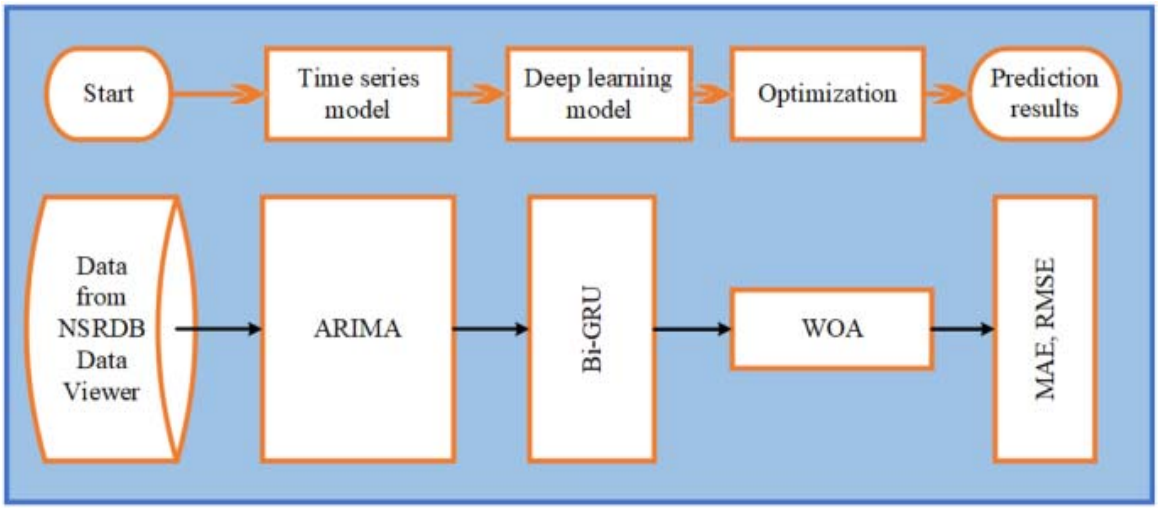

Fig. 3. Procedure for the proposed model

Auto Regressive Integrated Moving Average Model

The model comprises three components: Autoregressive (AR), Integrated (I), and Moving Average (MA) parts. It is essential for the considered time series data to be stationary to apply the ARIMA model [41].

$$X_t = \text{constant} + \sum_{k=1}^{m} P_k X_{t-k} + \sum_{k=1}^{n} A_k \varepsilon_{t-k} + \varepsilon_t + \sum_{k=1}^{o} D_k d_{t-k} \quad (1)$$

The Augmented Dickey-Fuller (ADF) test validates the data, which produced m, n, and o values. The AR (m) and MA (n) values were determined using the Partial Autocorrelation Function (PACF) and the Autocorrelation Function (ACF) functions. The 'o' value is determined by differencing the data.

Bidirectional – Gate Recurrent Unit Model

In [39], the Gated Recurrent Unit is a variant of Recurrent Neural Networks that efficiently addresses the issue of gradient vanishing in standard RNNs while maintaining the memory function of Long Short-Term Memory. Another advantage of GRU is that it runs faster because of fewer parameters during the training phase. GRU uses two gates, the reset gate and the update gate, to govern the flow of information within the network as shown in Fig. 4. These gates are critical in decision-making for information preservation and writing into the candidate's memory state. The update gate specifies the degree to which the previous hidden layer state p(t-1) influences the present state p(t). GRU uses the activation function to process

data from p(t-1) and the present moment a(t). The activation result z(t) is smaller, the more information is preserved [42].

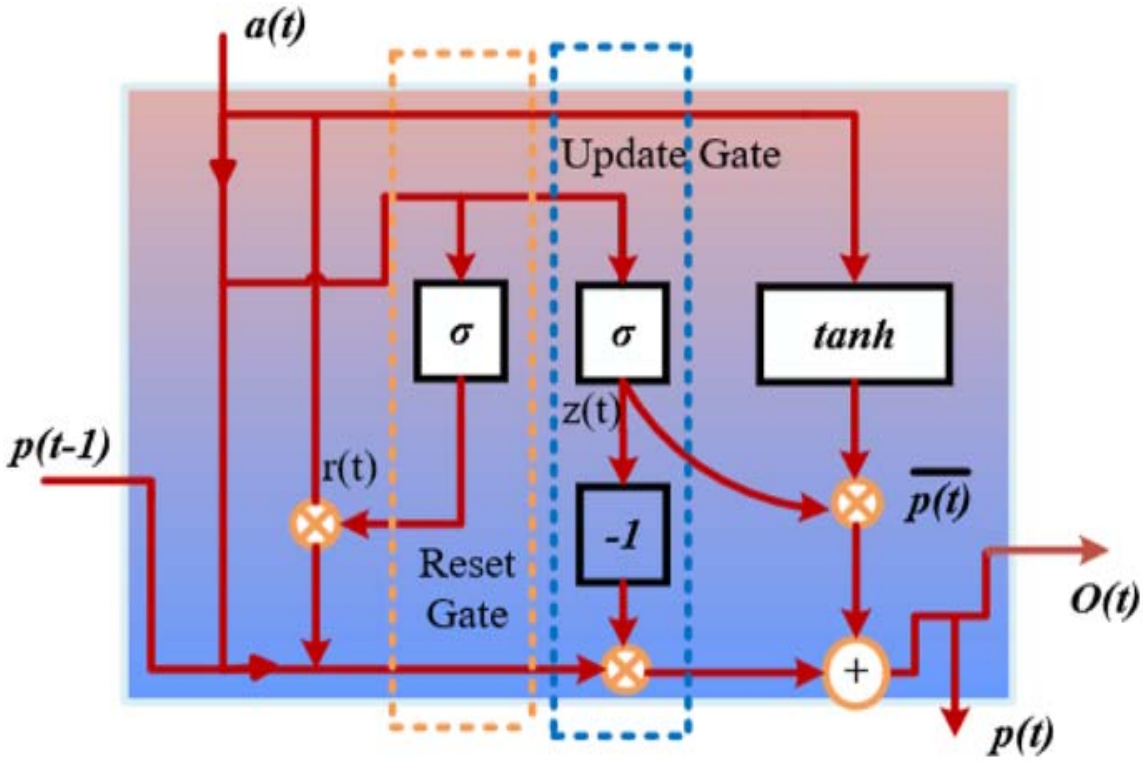

Fig. 4. Internal structure of a Gate recurrent unit cell

$$r(t) = \sigma\left(w_r^T [p(t-1), a(t)] + b_r\right) \tag{2}$$

$$z(t) = \sigma\left(w_z^T . [p(t-1), a(t)] + b_z\right) \tag{3}$$

$$\tilde{p}(t) = \mathrm{Tanh}\left(w_p^T x(t) + w_p^T (r(t) \odot p(t-1))\right) + b_p \tag{4}$$

Bi–GRU is formed by combining two layers of GRUs, each working in a different information transmission direction as shown in Fig. 5. This bidirectional technique ensures that the model examines both past and future data. The Bi–GRU architecture adds a reverse layer to the one-layer GRU network to capture input information from both ways. Bi–GRU's use of two hidden layers is a key feature, allowing it to extract past and future information [43]. These two hidden layers, capturing information from different temporal perspectives, are intricately linked to a shared output layer.

$$p(t) = (1 - z(t)) \odot p(t-1) + z(t) \odot \tilde{p}(t) \tag{5}$$

$$p'(t) = \left(1 - z'^{(t)}\right) \odot p'(t-1) + z'(t) \odot \tilde{p'}(t) \tag{6}$$

$$p''(t) = p'(t) + p(t) \tag{7}$$

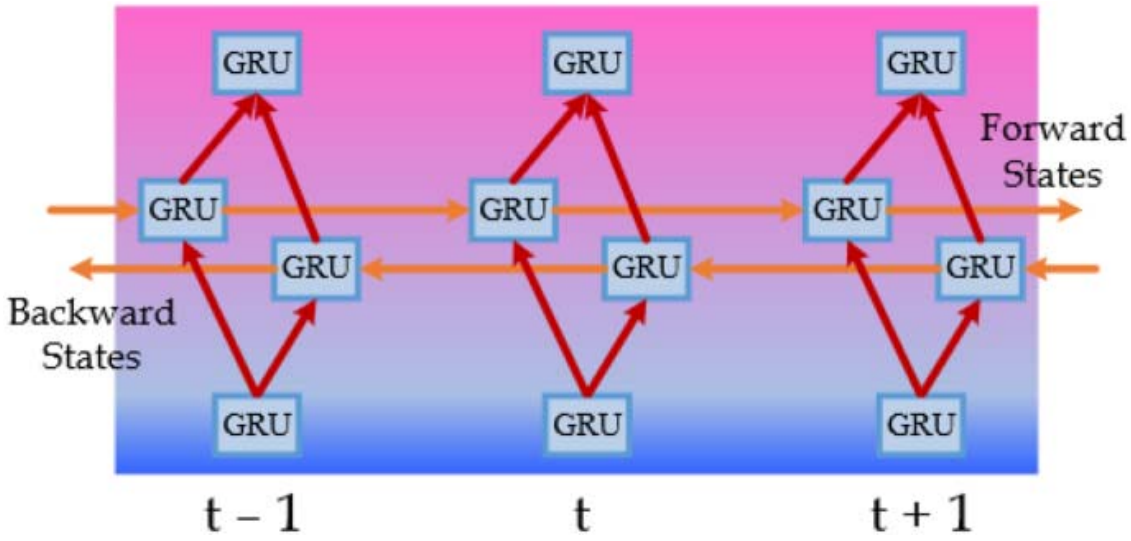

Fig. 5. Structure of Bi-directional gate recurrent unit

This bidirectional configuration enhances the model's capacity to comprehend and utilize a more comprehensive set of temporal dependencies, ultimately contributing to improved predictive performance.

Whale Optimization Model

The main goal of the optimization model is to teach a deep learning system to find the best neuron number and learning rate that minimizes prediction errors [44]. Humpback whales target krill and small fish herds. They release bubbles in spirals around their prey and then swim upwards towards the surface. The process works in three stages in the Fig. 6 [45].

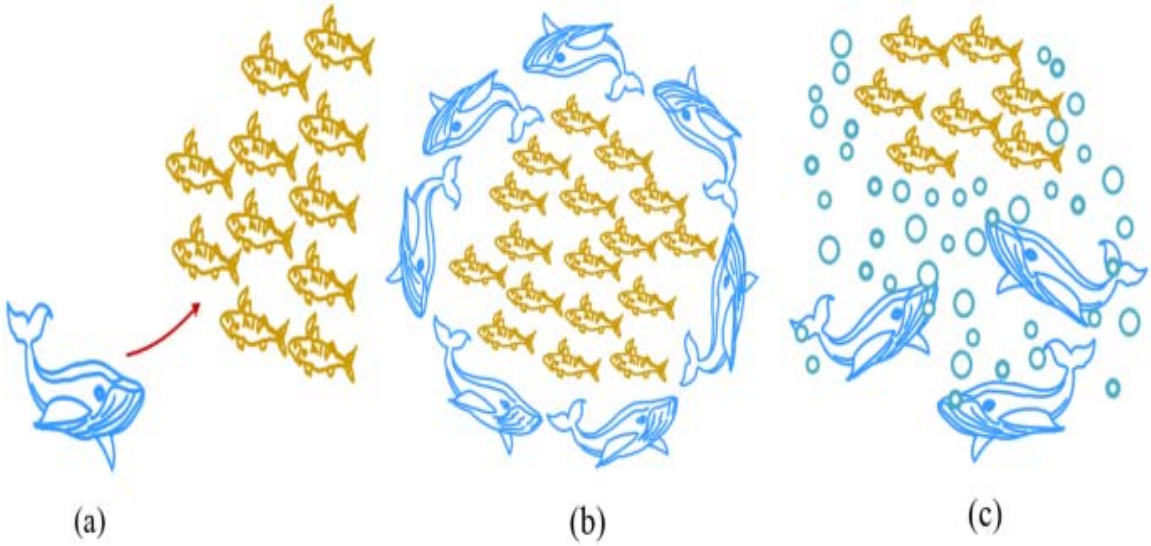

Fig. 6. Hunting process of prey by whale optimization algorithm

Encircling Prey

In the first stage of WOA, Whales choose the best solution (like the best guess) and have other options to adjust their positions toward it [46].

Attacking Prey

In the second stage, WOA has two ways to approach the prey. One is gradually closing in on the target by adjusting positions around it. The other is by spiraling around the prey until we get closer.

Exploration for Prey

In the final stage, WOA explores without getting stuck at local minima, and aims to find the best solution globally [47].

Results

Table 1 shows the autoregressive, moving average, and differencing parameters for the eight PSS locations obtained from the ADF test. These parameters are fitted in the ARIMA model and residuals are obtained. The residuals are passed thereby into the Bi – GRU – WOA model. The hyperparameters for the eight PSS locations are obtained from the whale optimization algorithm and are presented in Table 1. The same procedure is repeated, and the results are taken with other optimization models including the Regular model (100 neurons and 0.01 learning rate), the Genetic algorithm, Whale optimization, and Particle swarm optimization algorithms with a 7:3 train/test ratio. All the models are run for 100 epochs and a batch size (BS) of 64 with learning rate (LR) and neuron number (NN) optimized. Mean Absolute Error (MAE) and Root Mean Square Error (RMSE) are used as metrics [48] to analyze the performance of the models involved in the work.

Various deep learning models are compared with Root mean square error in Table 2 with ARIMA – Bi – GRU performing best with low RMSE value. Hence, the ARIMA – Bi – GRU model is optimized with various optimization techniques to enhance the prediction results. The results of all these optimization techniques applied to the proposed model are compared in Fig. 7. The graph is spread in all directions, closer to the center indicating less error and far from the center presenting a high error.

Table 1. Solar irradiance forecasting by ARIMA – Bi – GRU – WOA model

Season	Data	Model	ADF Test (m, n, o)	Parameters (NN, LR)	Metrics		
					Mean	MAE	RMSE
PSS1	1,84,085	ARIMA – Bi – GRU – WOA	(2, 0, 2)	(83, 0.008)	221.0	2.16	2.53
PSS2	1,84,085		(2, 0, 2)	(74, 0.01)	213.0	2.53	5.48
PSS3	1,84,085		(2, 0, 2)	(77, 0.01)	207.6	1.81	5.74
PSS4	1,84,085		(2, 0, 2)	(97, 0.009)	205.6	2.24	6.64
PSS5	1,84,085		(2, 0, 2)	(71, 0.007)	210.1	3.63	9.51
PSS6	1,84,085		(2, 0, 2)	(87, 0.01)	216.3	0.34	0.75
PSS7	1,84,085		(2, 0, 2)	(99, 0.01)	221.1	2.51	5.45
PSS8	1,84,085		(2, 0, 2)	(72, 0.01)	191.1	2.07	2.43

Table 2. Comparison of RMSE errors for the deep learning models for sample location

Model	LSTM	GRU	Bi – LSTM	Bi – GRU	ARIMA – Bi – GRU
RMSE (W/m^2)	2.83	2.75	2.80	2.73	1.58

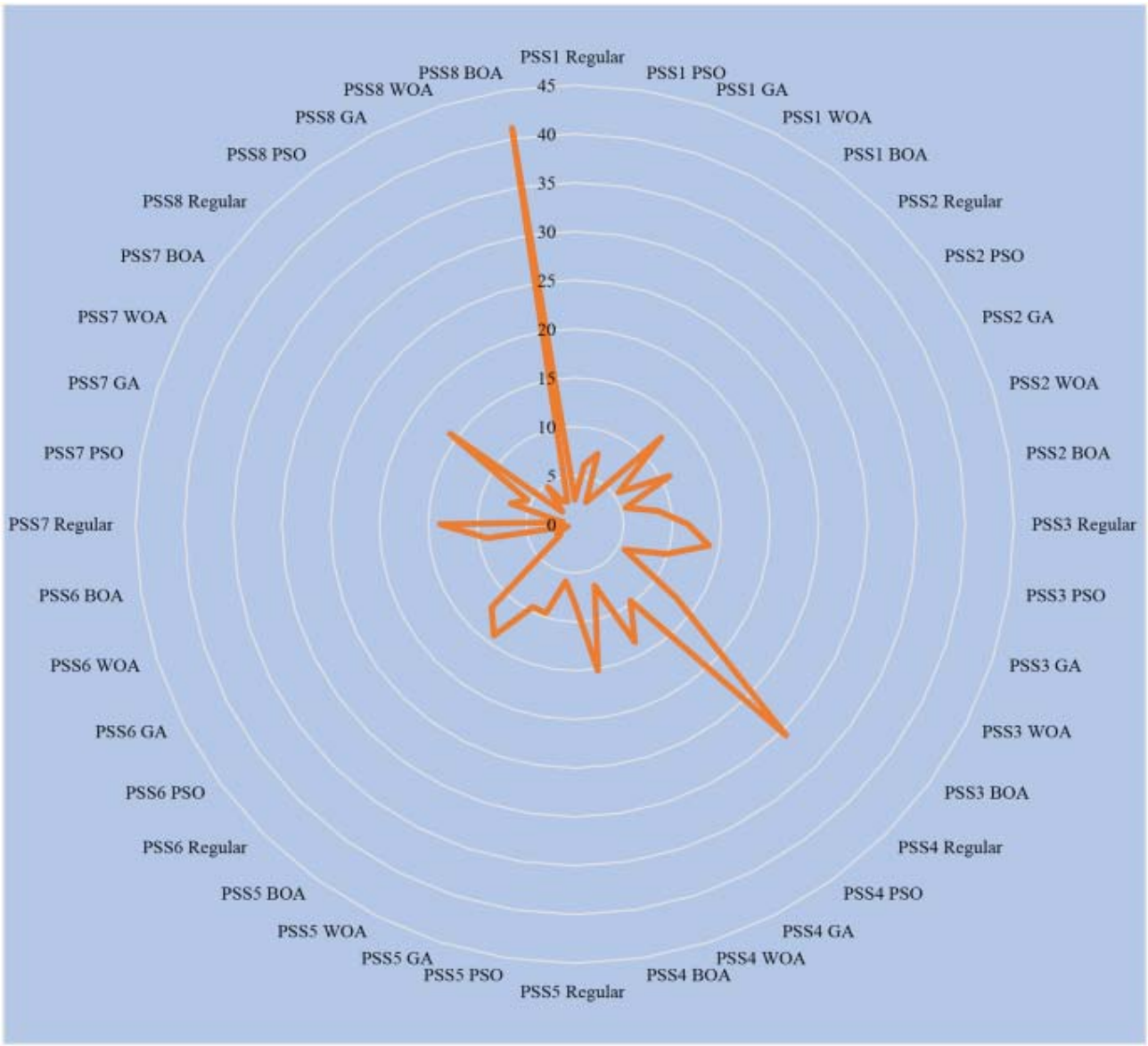

Fig. 7. Comparison of RMSE values for optimization models for ARIMA – Bi – GRU

From Fig. 7, it is observed that for the first location, the regular optimization for the proposed model achieves the lowest RMSE error of 2.51 W/m², followed by WOA, BOA, PSO, and GA optimizations with values of 2.53, 4.01, 6.51, and 7.57 W/m², respectively. In the second location, the WOA model performs best with an RMSE of 5.48 W/m², followed by PSO, BOA, GA, and the regular model with values of 5.56, 8.65, 10.9, and 12.55 W/m², respectively. For the third location, the WOA model also shows superior performance with an RMSE of 5.74 W/m², followed by GA, the regular model, BOA, and PSO with values of 9.89, 11.6,

12.89, and 13.94 W/m², respectively. In the fourth location, WOA again performs best with an RMSE of 6.64 W/m², followed by PSO, GA, BO, and the regular model with values of 9.69, 13.57, 15.22, and 30.6 W/m², respectively.

For the fifth location, PSO demonstrates the best results with an RMSE of 5.93 W/m², followed by the regular model, WOA, GA, and BOA with values of 8.12, 9.51, 9.58, and 14.1 W/m², respectively. The sixth location results also highlight WOA as the top performer with an RMSE of 0.75 W/m², followed by PSO, GA, BOA, and the regular model with values of 1.8, 2.06, 9.09, and 12.05 W/m², respectively. In the seventh location, PSO outperforms the other models with an RMSE of 1.21 W/m², followed by WOA, GA, the regular model, and BOA with values of 5.45, 6.9, 13.8, and 15.8 W/m², respectively. Finally, in the eighth location, the regular model achieves the best performance with an RMSE of 1.8 W/m², followed by WOA, GA, PSO, and BOA with values of 2.43, 2.66, 4.75, and 41.1 W/m², respectively. Comparing the results, the WOA model shows better generalization across all locations compared to the other optimization algorithms for the proposed ARIMA – Bi – GRU model. Since the performance of ARIMA – Bi – GRU – WOA is better than any other model discussed, the findings (analytical and visual presentations) for all eight PSS locations are detailed in Table 1 and illustrated in Figs. 8 and 9. Figure 8 shows the solar irradiance variation to sample number based on date and time. The Y axis is the Solar irradiance actual and predicted in W/m^2 whereas the X axis is the Sample number based on date and time. Similarly, Fig. 9 shows the error variation in sample number based on date and time. The Y axis is the error and rolling mean error in W/m^2 whereas the X axis is the Sample number based on date and time. The statistical performance of the proposed model, as shown in Table 1, indicates mean absolute errors ranging from 0.34 to 3.63 W/m², and root mean square errors ranging from 0.75 to 9.51 W/m^2, depending on the location.

Conclusion

This research focused on accurately predicting solar irradiance to provide valuable data for effective solar energy harnessing, particularly on Pumped Storage Hydroelectric Power Plants. The comprehensive experimentation and analysis demonstrate the superiority of the ARIMA-Bi-GRU hybrid model, highlighting its effectiveness in optimizing solar irradiance predictions for the hydro system. The proposed model demonstrated commendable performance, with the Whale optimization technique proving the most effective, while Bayesian optimization exhibited relatively less efficacy. The analysis revealed that PSS 1 with average solar irradiance of 221.0 W/ m^2 and PSS 7 with 221.1 W/ m^2 are the optimal locations, achieving the highest mean solar irradiation among the eight designated sites. The RMSE values exhibited variation, ranging from 0.75 to 9.51 W/ m^2 for the ARIMA – Bi – GRU – WOA model, depending on the location of the PSS. Considering only PSS1 and PSS7, the WOA performed with MAE 2.16 W/ m^2, RMSE 2.53 W/ m^2 and MAE 2.51 W/ m^2, RMSE 5.45 W/ m^{2,} respectively. The whale optimization technique contributes to the model's robust performance, marking a significant step forward in advancing sustainable energy solutions.

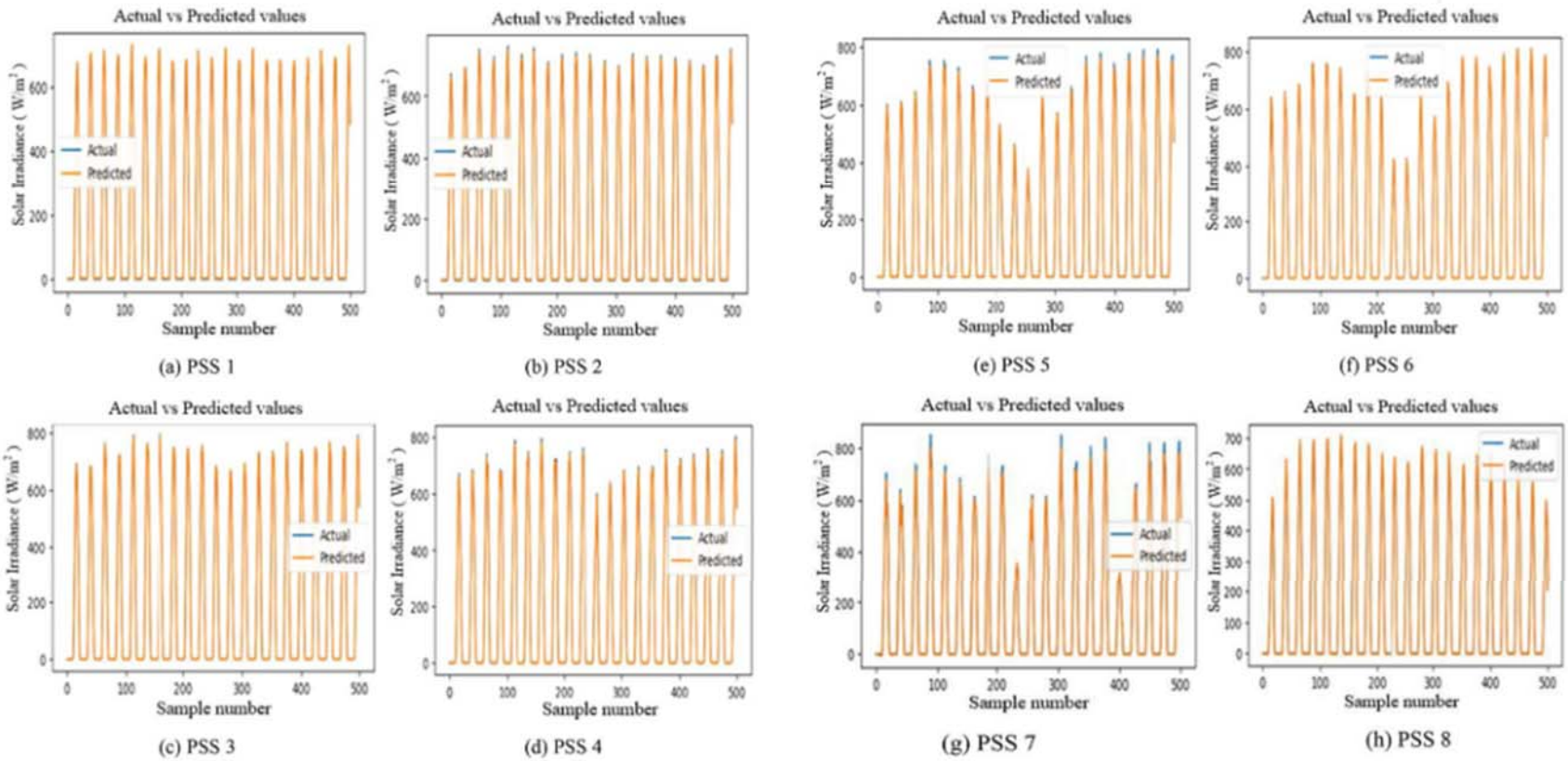

Fig. 8. Solar irradiance forecasting using ARIMA – Bi – GRU – WOA model

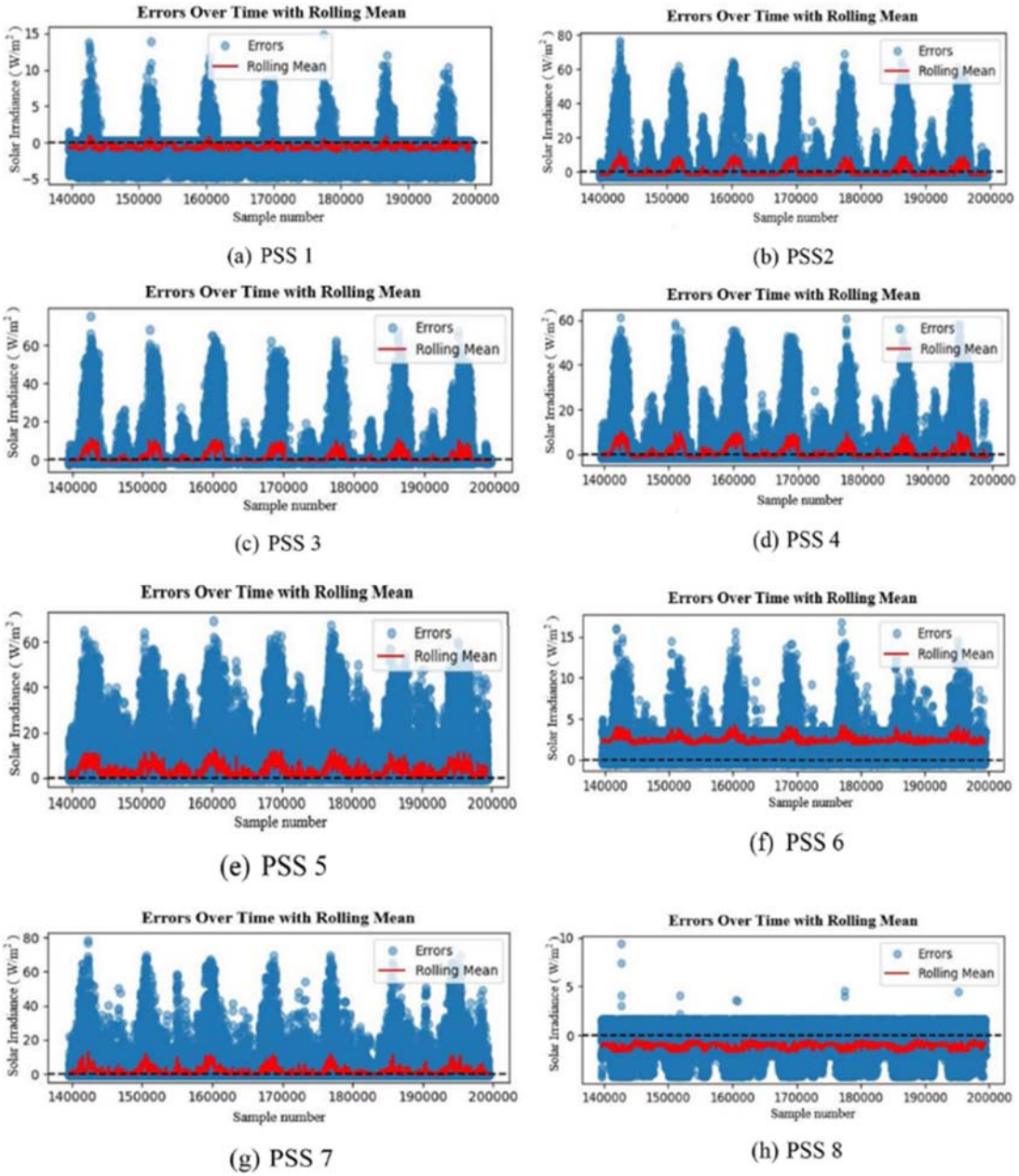

Fig. 9. Error analysis for eight PSS locations for the ARIMA – Bi – GRU – WOA model

The error observations show that the RMSE and MAE values vary by site as the data change. Each site has different errors, resulting in different predictive performance at various sites. This is because the study applies the model to individual site data, which reduces the overall accuracy of the proposed approach. The recommended solution is to use the model to combined data formed by pooling samples from each site and including the latitude and longitude of the sites as additional features. This approach would provide an average irradiance for each site with consistent errors and allow a more accurate assessment of high average solar irradiance. Extending the prediction to various multipurpose dams, storage facilities, and run-of-river systems with ponds also offers great potential to improve the availability and utilization of renewable energy.

Funding

NA.

Contributions

Sudharshan Konduru collected data, interpreted results, and wrote the paper. Naveeen C. set the objective of research work, developed methodology, carried out literature review and wrote the paper. R.C. Bansal reviewed and edited the paper and corresponding author of the paper.

Ethical Approval

NA.

Consent to Participate

NA.

Consent for Publication

Yes.

Competing Interests

The authors declare no competing interests.

Data Availability

No datasets were generated or analysed during the current study.

Code Availability

NA.

References

1. Raghuwanshi SS, Arya R (2019) Renewable energy potential in India and future agenda of research, International Journal of Sustainable Engineering, vol. 12, no. 5, pp. 1–12, Sep. https://doi.org/10.1080/19397038.2019.1602174
2. Harinarayana T, Kashyap KJ (2014) Solar Energy Generation potential estimation in India and Gujarat, Andhra, Telangana States. Smart Grid Renew Energy 5(11):275–289. https://doi.org/10.4236/sgre.2014.511025
3. Ramachandra TV, Jain R, Krishnadas G (2011) Hotspots of solar potential in India. Renew Sustain Energy Rev 15(6):3178–3186. https://doi.org/10.1016/j.rser.2011.04.007
4. Solomin E, Sirotkin E, Cuce E, Selvanathan SP, Kumarasamy S, Energies (2021) 14, 10, pp. 1–25, https://doi.org/10.3390/en14102751
5. Kumar P et al (Jan. 2024) Efficient integration of photo voltaic and hydro energy technologies for sustainable power generation in rural areas: a case study. Mater Sci Energy Technol 7:297–308. https://doi.org/10.1016/J.MSET.2024.04.002

6. Khare V, Jain A, Bhuiyan MA (Dec. 2023) Assessment of hydro energy potential from rain fall data set in India through data analysis. e-Prime - Adv Electr Eng 6. Electronics and Energy10.1016/j.prime.2023.100290
7. IRENA (2024) Renewable energy statistics 2024. International Renewable Energy Agency, Abu Dhabi. https://www.irena.org/. Accessed 10 Jun 2024
8. Kumar D, Katoch SS (Jul. 2014) Sustainability indicators for run of the river (RoR) hydropower projects in hydro rich regions of India. Renew Sustain Energy Rev 35:101–108. https://doi.org/10.1016/J.RSER.2014.03.048
9. Mahfoud RJ, Alkayem NF, Zhang Y, Zheng Y, Sun Y, Alhelou HH (May 2023) Optimal operation of pumped hydro storage-based energy systems: a compendium of current challenges and future perspectives. Renew Sustain Energy Rev 178:113267. https://doi.org/10.1016/J.RSER.2023.113267
10. Parikh JK, Magotra R, Panda RR (2020) Role of pumped hydro energy storage in India's renewable transition, Accessed: Feb. 08, 2024. [Online]. Available: https://irade.org/TAF%20Final%20Report.pdf
11. Koritarov V, Kwon J, Ploussard Q, Balducci P (2022) Review of technology innovations for pumped storage hydropower, pp. 25–154, Apr. Accessed: Feb. 08, 2024. [Online]. Available: https://publications.anl.gov/anlpubs/2022/05/175341.pdf
12. Toufani P, Karakoyun EC, Nadar E, Fosso OB, Kocaman AS (2023) Optimization of pumped hydro energy storage systems under uncertainty: A review, Dec. 20, *Elsevier Ltd*. https://doi.org/10.1016/j.est.2023.109306
13. Bhimaraju A, Mahesh A, Nirbheram JS (2023) Feasibility study of solar photovoltaic/grid-connected hybrid renewable energy system with pumped storage hydropower system using abandoned open cast coal mine: A case study in India, *J. Energy Storage*, vol. 72, p. 108206, Nov. https://doi.org/10.1016/J.EST.2023.108206
14. Singh RK (2023) Ongoing hydro-power projects, Government of India Ministry of Power, Lok Sabha, Mar. Accessed: Feb. 08, 2024. [Online]. Available: https://powermin.gov.in/
15. Bansal RC, Bhatti TS (2008) Small signal analysis of isolated hybrid power systems: reactive power and frequency control analysis. Alpha Science International, Oxford, U.K.
16. Wen S, Zhang C, Lan H, Xu Y, Tang Y, Huang Y (Jan. 2021) A hybrid ensemble model for interval prediction of solar power output in ship onboard power systems. IEEE Trans Sustain Energy 12(1):14–24. https://doi.org/10.1109/TSTE.2019.2963270
17. Saini D, Saxena A, Bansal RC (2016) Electricity price forecasting by linear regression and SVM. Int Conf Recent Adv Innovations Eng ICRAIE. https://doi.org/10.1109/ICRAIE.2016.7939509
18. Yang B et al (2023) Classification and Summarization of Solar Irradiance and Power Forecasting Methods: A Thorough Review, May 01, *China Electric Power Research Institute*. https://doi.org/10.17775/CSEEJPES.2020.04930
19. Almarzooqi AM, Maalouf M, El-Fouly THM, Katzourakis VE, El Moursi MS, Chrysikopoulos CV (2024) A hybrid machine-learning model for solar irradiance forecasting, *Clean Energy*, vol. 8, no. 1, pp. 100–110, Feb. https://doi.org/10.1093/CE/ZKAD075
20. Wen H, Du Y, Chen X, Lim EG, Wen H, Yan K (Nov. 2023) A regional solar forecasting approach using generative adversarial networks with solar irradiance maps. Renew Energy 216:119043. https://doi.org/10.1016/J.RENENE.2023.119043
21. Ok D, Pu Y, Incecik A (2007) Artificial neural networks and their application to assessment of ultimate strength of plates with pitting corrosion, *Ocean Engineering*,

vol. 34, no. 17–18, pp. 2222–2230, Dec. https://doi.org/10.1016/j.oceaneng.2007.06.007
22. Bansal RC, Pandey JC (2005) Load forecasting using artificial intelligence techniques: a literature survey. Int J Comput Appl Technol 22:2–3. https://doi.org/10.1504/IJCAT.2005.006942
23. Chu Y, Li M, Coimbra CFM, Feng D, Wang H (Oct. 2021) Intra-hour irradiance forecasting techniques for solar power integration: a review. iScience 24(10):103136. https://doi.org/10.1016/J.ISCI.2021.103136
24. Prema V, Bhaskar MS, Almakhles D, Gowtham N, Rao KU (2021) Critical review of data, models and performance metrics for wind and solar power forecast. IEEE Access 10:667–688. https://doi.org/10.1109/ACCESS.2021.3137419
25. Babu CN, Reddy BE (Oct. 2014) A moving-average filter based hybrid ARIMA–ANN model for forecasting time series data. Appl Soft Comput 23:27–38. https://doi.org/10.1016/J.ASOC.2014.05.028
26. Sujil A, Kumar R, Bansal RC (2019) FCM clustering-ANFIS-based PV and wind generation forecasting agent for energy management in a smart microgrid, *The Journal of Engineering*, vol. no. 18, pp. 4852–4857, Jul. 2019, https://doi.org/10.1049/JOE.2018.9323
27. Madhiarasan M, Deepa SN (2016) Deep neural network using new training strategy based forecasting method for wind speed and solar irradiance forecast. Middle-East J Sci Res 24(12):3730–3747. https://doi.org/10.5829/idosi.mejsr.2016.3730.3747
28. Zhao Y, Dong S, Jiang F, Incecik A (Mar. 2021) Mooring tension prediction based on BP neural network for semi-submersible platform. Ocean Eng 223. https://doi.org/10.1016/j.oceaneng.2021.108714
29. Kumar D, Mathur HD, Bhanot S, Bansal RC (2021) Forecasting of solar and wind power using LSTM RNN for load frequency control in isolated microgrid. Int J Model Simul 41(4):311–323. https://doi.org/10.1080/02286203.2020.1767840
30. Poti KD, Naidoo RM, Mbungu NT, Bansal RC (2023) Intelligent solar photovoltaic power forecasting, *Energy Reports*, vol. 9, pp. 343–352, Oct. https://doi.org/10.1016/J.EGYR.2023.09.004
31. da Silva DG, de Meneses AA (2023) Comparing long short-term memory (LSTM) and bidirectional LSTM deep neural networks for power consumption prediction, *Energy Reports*, vol. 10, pp. 3315–3334, Nov. https://doi.org/10.1016/j.egyr.2023.09.175
32. Huang Z, Yang F, Xu F, Song X, Tsui KL (2019) Convolutional gated recurrent unit-recurrent neural network for state-of-charge estimation of Lithium-ion batteries. IEEE Access 7:93139–93149. https://doi.org/10.1109/ACCESS.2019.2928037
33. Kumari P, Toshniwal D (2021) Deep learning models for solar irradiance forecasting: A comprehensive review, Oct. 10, *Elsevier Ltd*. https://doi.org/10.1016/j.jclepro.2021.128566
34. Fang Z, Dowe DL, Peiris S, Rosadi D (2021) Minimum message length in hybrid arma and lstm model forecasting, *Entropy*, vol. 23, no. 12, Dec. https://doi.org/10.3390/e23121601
35. Zhang W, Lin Z, Liu X (2022) Short-term offshore wind power forecasting - A hybrid model based on Discrete Wavelet Transform (DWT), Seasonal Autoregressive Integrated Moving Average (SARIMA), and deep-learning-based Long Short-Term Memory (LSTM), *Renew Energy*, vol. 185, pp. 611–628, Feb. https://doi.org/10.1016/j.renene.2021.12.100
36. Luo J, Gong Y (Jun. 2023) Air pollutant prediction based on ARIMA-WOA-LSTM model. Atmos Pollut Res 14(6). https://doi.org/10.1016/j.apr.2023.101761

37. Hazra S, Roy PK (2021) Renewable energy incorporating short-term optimal operation using oppositional grasshopper optimization, *Optim Control Appl Methods*, vol. 44, no. 2, pp. 452–479, Oct
38. Hazra S, Roy PK (2023) Solar-wind-hydro-thermal scheduling using moth flame optimization, *Optim Control Appl Methods*, vol. 44, no. 2, pp. 391–425, Mar. https://doi.org/10.1002/oca.2783
39. Hazra S, Roy PK, Paul C (2024) State of the art for moth-flame optimization applied electric vehicles–solar–wind–hydro–thermal power system. Electr Eng. https://doi.org/10.1007/s00202-024-02573-8
40. POWER | DAVe Accessed: Jun. 10, 2024. [Online]. Available: https://power.larc.nasa.gov/data-access-viewer/
41. Marhic B, Masson J-B Occupancy forecasting using two ARIMA strategies energy management view project smart heating view project. [Online]. Available: https://www.researchgate.net/publication/336553179
42. Liu Y et al (Nov. 2019) Ensemble spatiotemporal forecasting of solar irradiation using variational bayesian convolutional gate recurrent unit network. Appl Energy 253. https://doi.org/10.1016/j.apenergy.2019.113596
43. Rai A, Shrivastava A, Jana KC (Feb. 2022) A robust auto encoder-gated recurrent unit (AE-GRU) based deep learning approach for short term solar power forecasting. Optik (Stuttg) 252. https://doi.org/10.1016/j.ijleo.2021.168515
44. Yang R, Yuan Y, Ying R, Shen B, Long T (Mar. 2020) A novel energy management strategy for a ship's hybrid solar energy generation system using a particle swarm optimization algorithm. Energies (Basel) 13(3). https://doi.org/10.3390/en13061380
45. Syama S, Ramprabhakar J, Anand R, Guerrero JM (Sep. 2023) A hybrid extreme learning machine model with Lévy flight chaotic Whale optimization algorithm for wind speed forecasting. Results Eng p. 101274. https://doi.org/10.1016/j.rineng.2023.101274
46. Cheng J, Xu J, Chen W, Song B (2022) Locating and sizing method of electric vehicle charging station based on Improved Whale Optimization Algorithm, *Energy Reports*, vol. 8, pp. 4386–4400, Nov. https://doi.org/10.1016/j.egyr.2022.03.077
47. Jafari M, Chaleshtari MHB, Khoramishad H, Altenbach H (Jan. 2023) Minimization of thermal stress in perforated composite plate using metaheuristic algorithms WOA, SCA and GA. Compos Struct 304. https://doi.org/10.1016/j.compstruct.2022.116403
48. Prema V, Bhaskar MS, Almakhles D, Gowtham N, Rao KU (2022) Critical review of data, models and performance metrics for wind and solar power forecast. Inst Electr Electron Eng Inc. https://doi.org/10.1109/ACCESS.2021.3137419